PAPER

Redox-active nickel and cobalt tris(pyrazolyl)borate dithiocarbamate complexes: air-stable Co(II) dithiocarbamates†

David J. Harding,*[a] Phimphaka Harding,[a] Supaporn Dokmaisrijan[a] and Harry Adams[b]

A series of new cobalt(II) and nickel(II) tris(3,5-diphenylpyrazolyl)borate (Tp^{Ph2}) dithiocarbamate complexes [Tp^{Ph2}M(dtc)] (M = Co, dtc = S$_2$CNEt$_2$ **1**, S$_2$CNBz$_2$ **2** and S$_2$CN(CH$_2$)$_4$ **3**; M = Ni, dtc = S$_2$CNEt$_2$ **4**, S$_2$CNBz$_2$ **5** and S$_2$CN(CH$_2$)$_4$ **6**) have been prepared by the reaction of [Tp^{Ph2}MBr] with Nadtc in CH$_2$Cl$_2$. IR spectroscopy indicates that the Tp^{Ph2} ligand is κ^3 coordinated while the dithiocarbamate ligand is κ^2 coordinated. ^{1}H NMR and UV-Vis spectroscopy are consistent with high spin, five-coordinate metal centres. X-ray crystallographic studies of **1**, **3** and **6** confirm the κ^3 coordination of the Tp^{Ph2} ligand and reveal an intermediate five-coordinate geometry with an asymmetrically coordinated dithiocarbamate ligand. Electrochemical studies of **1–6** reveal a metal centred *reversible* one-electron oxidation to M(III). Attempted oxidation of [Tp^{Ph2}Co(dtc)] with [FeCpCp^{COMe}]BF$_4$ yields [Co(dtc)$_3$], Hpz^{Ph2} and a further product which may be [Tp^{Ph2}CoBp^{Ph2}]. DFT calculations indicate that the low redox potentials in these complexes result from a strongly antibonding M–S σ* HOMO.

Introduction

Tris(pyrazolyl)borates, Tp^R (R denotes substituents on the pyrazole rings) are one of the most widely used facially capping ligands in coordination chemistry.[1,2] Their popularity arises from their ease of synthesis and the readiness with which their steric and electronic properties may be varied by altering the substituents on the pyrazole rings.[1] While Tp and Tp^{Me2} are widely used in the preparation of half-sandwich complexes of second and third row transition metals, with first row transition metals chemically inert sandwich compounds [Tp$_2$M] form.[1] However, by employing sterically hindered scorpionates such as Tp^{t-Bu}, Tp^{Ph} and Tp^{i-Pr} half-sandwich complexes [Tp^{R}MX] (X = halide or pseudohalide) can be prepared.[3–6] Thus, [Tp^{R}CoL] (L = anionic ligand) complexes have been prepared as spectroscopic probes for the zinc analogues [Tp^{R}Zn(L)] and structural and functional models for the native zinc enzymes.[7–10] Cobalt and nickel thiolate complexes, [Tp^{R}M(SR')] have also been prepared to provide insight into how the subtle differences between cobalt, nickel and copper affect the reactivity of the copper models for blue copper proteins.[11–13] Furthermore, Akita and co-workers have synthesized numerous organometallic species [Tp^{R}MR] (M = Co, Ni; R = allyl, alkyl, aryl or alkynyl) to provide insight into catalytic transformations or for

use as polymerization catalysts.[14–17] Finally, [Tp^{Ph,Me}M(Hpz^{Ph,Me})L] (M = Co, Ni; L = 2,6-di-*tert*-butyl-4-carboxyphenoxide) have been synthesized in an attempt to prepare molecular magnets.[18]

Despite the wealth of research into cobalt and nickel tris(pyrazolyl)borate complexes the redox chemistry of these systems remains extremely poorly developed. Theopold has shown that the reduction of [Tp$^{t-Bu,Me}$CoI] with magnesium gives [Tp$^{t-Bu,Me}$Co(N$_2$)] which then undergoes a wide range of reactions to form [Tp$^{t-Bu,Me}$Co(L)] (L = CO, alkene) or [Tp$^{t-Bu,Me}$CoX] (X = Cl, OH, H).[19–21] The oxidation of [{Tp^{R}M}$_2$(μ-OH)$_2$] (M = Co, Ni; R = Me$_2$, Me$_3$, *i*-Pr$_2$) has also been explored by Akita *et al.*[22] More recently, work in our group has extended the number of such redox-active complexes to include a series of cobalt complexes, [Tp^{Ph2}Co(β-dkt)] (β-dkt = β-diketonate) which undergo irreversible oxidation.[23] Lastly, a new series of nickel dithiocarbamate complexes, [Tp^{R}Ni(dtc)] (R = Me$_2$; Ph,Me; dtc = dithiocarbamate) have been prepared by Jensen *et al.* with quasi-reversible oxidation being observed in all cases.[24–25] As part of our continuing interest in redox-active tris(pyrazolyl)borate complexes supported by the poorly represented Tp^{Ph2} ligand we have undertaken a study of cobalt and nickel dithiocarbamate Tp^{Ph2} complexes and their redox chemistry. Our findings are reported in the following paper.

## Results and discussion

Synthesis and characterisation

The reaction of [Tp^{Ph2}MBr] (M = Co or Ni) with NaS$_2$CNR$_2$ (R = Et, Bz) or NaS$_2$CN(CH$_2$)$_4$ in CH$_2$Cl$_2$ gave the expected dithiocarbamate complexes [Tp^{Ph2}M(S$_2$CNR$_2$)] (M = Co, R = Et

[a]Molecular Technology Research Unit, School of Science, Walailak University, Thasala, Nakhon Si Thammarat, 80161, Thailand. E-mail: hdavid@wu.ac.th; Fax: +66-75-672004; Tel: +66-75-672094
[b]Department of Chemistry, University of Sheffield, Brook Hill, Sheffield, S3 7HF, UK

† CCDC reference numbers 789217–789219. For crystallographic data in CIF or other electronic format see DOI: 10.1039/c0dt01010c

1, Bz **2**; M = Ni, R = Et **4**, Bz **5**) and [Tp^{Ph2}M(S$_2$Cpyr)] (M = Co **3**, Ni **6**) in good or excellent yields as purple-brown (M = Co) or green (M = Ni) solids (Scheme 1).
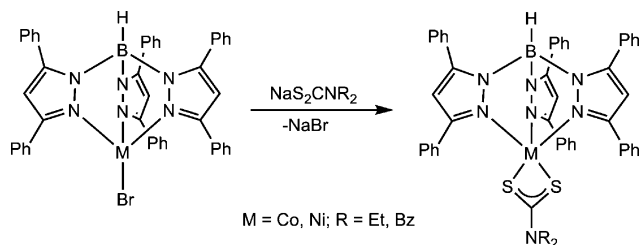
Scheme 1   Synthesis of [Tp^{Ph2}M(dtc)] **1**, **2**, **4**, **5**.

The compounds are soluble in polar organic solvents such as CH$_2$Cl$_2$ and acetone. Successful synthesis of the cobalt complexes requires longer reaction times than the corresponding nickel complexes, typically 5–6 h compared with 2 h, as [Tp^{Ph2}CoBr] is only sparingly soluble in CH$_2$Cl$_2$ while [Tp^{Ph2}NiBr] dissolves readily. The synthesis of the air-stable cobalt(II) dithiocarbamate complexes, **1–3**, is particularly notable as cobalt(II) dithiocarbamate complexes are comparatively rare and usually highly susceptible to oxidation.[26] Moreover, while **1–3** are readily synthesized attempts to prepare the Tp^{Ph,Me} analogues under the same conditions led to a complex mixture of products including the cobalt(III) tris(dithiocarbamate) complexes, [Co(dtc)$_3$], suggesting that the electron poor Tp^{Ph2} ligand is vital to the successful synthesis of stable Co(II) dithiocarbamate compounds.

IR spectroscopy reveals B–H stretches between 2610 and 2626 cm^{-1} indicative of κ^3 coordinated Tp^{Ph2} ligands (Table 1). There are also very strong C–N stretches between 1479 and 1471 cm^{-1} confirming the presence of a dithiocarbamate ligand in the metal coordination sphere.[27] The corresponding C–S stretches are weak bands observed between 1011 and 1009 cm^{-1}. Similar stretches are observed in the closely related [Tp*Ni(dtc)] complexes.[24]

Solution UV-Vis spectra of **1–6** were recorded in CH$_2$Cl$_2$ and are shown in Fig. 1. In the case of the cobalt complexes there are two main features in the spectra one at *ca.* 400 nm and another between 505 and 535 nm. The former of these bands has a large molar extinction coefficient and by comparison with [Tp^{Ph,Me}Co(thiomaltolate)] which has a similar band at 391 nm is assigned as a sulfur-to-Co(II) LMCT band.[8] The other band is assigned to a d–d transition as the related five-coordinate complex [Tp^{i-Pr2}Co(SMeIm)] (SMeIm = 2-mercapto-1-methylimidazolate)

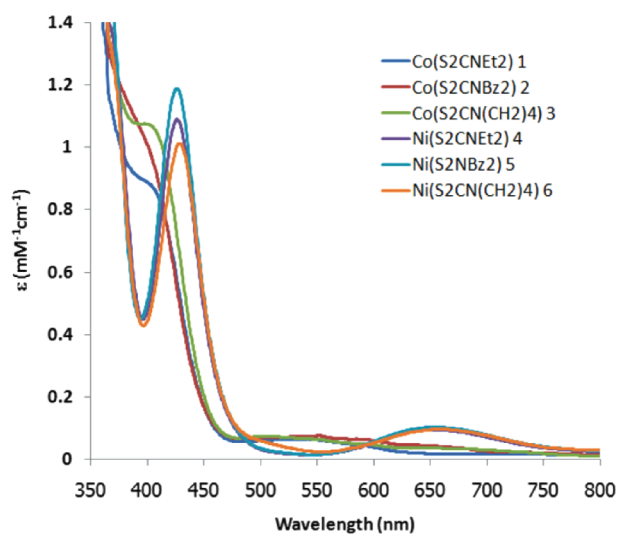**Fig. 1**   UV-Vis spectra of [Tp^{Ph2}M(dtc)].

has a band at 563 nm.[13] The analogous nickel complexes, **4–6** have two features: a shoulder at *ca.* 370 nm and further band between 426 and 429 nm indicative of sulfur-to-Ni(II) LMCT bands. For comparison, the recently reported [Tp^{Ph,Me}Ni(dtc)] (dtc = S$_2$CNEt$_2$, S$_2$CNPh$_2$) complexes also exhibit bands at 420 and 428 nm, respectively and in the case of [Tp^{Ph,Me}Ni(S$_2$CNEt$_2$)] a shoulder at 380 nm.[25] The CT bands at *ca.* 370 nm are thought to correspond to a S–Ni σ–σ* transition while the lower energy bands are caused by the S–metal π bond in accordance with the assignments made by Fujisawa *et al.* in the cobalt and nickel complexes [Tp^{i-Pr2}M(SMeIm)].[13]

Interestingly, while the cobalt complexes reveal a weak blue shift in going from **1** to **3** an opposite trend is observed for the nickel complexes, **4–6** where the band is red-shifted with decreasing *S*,*S*'-chelate donor strength. Furthermore, the sulfur-to-metal(II) CT bands of the cobalt series are found to be on average 22 nm lower than their nickel counterparts. A similar albeit larger shift is observed in [Tp*M(CysEt)] (M = Co, Ni, CysEt = L-cysteine ethyl ester) where the difference is 48 nm.[28,29] In addition to the above charge transfer bands there is also a d–d transition between 654 and 658 nm for **4–6**. Once again comparable bands are observed in previously reported [Tp^{R}Ni(dtc)] complexes.[24-25] Overall, the spectra are consistent with five-coordinate, high spin M(II) complexes.

Table 1   Physical, spectroscopic and electrochemical data for [Tp^{Ph2}M(dtc)] **1–6**

| Complex | Colour | Yield (%) | IR/cm^{-1a} | | | $E^{o'}$/V^b | λ$_{max}$/nm (ε/M^{-1} cm^{-1}) |
			ν_{BH}	ν_{CN}	ν_{CS}		
1	Purple-brown	63	2623	1478	1010	0.49	408 (859), 536 (63)
2	Purple-brown	69	2613	1475	1009	0.56	404 (974), 535 (72)
3	Purple	64	2626	1479	1011	0.54	402 (1,071), 505 (73)
4	Dark green	85	2624	1478	1011	0.57	372sh (1,460), 426 (1,190), 654 (95)
5	Dark green	84	2610	1471	1011	0.64	365sh (1,860), 426 (1,187), 655 (103)
6	Green	77	2626	1479	1011	0.62	372sh, (1,360), 429 (1,011), 658 (95)

^{a} As KBr discs ^{b} At 100 mV s^{-1} *versus* Ag/AgCl

Table 2 ^{1}H NMR spectroscopic data for [Tp^{Ph_2}M(dtc)] **1–6**^{a}

| Complex	Tp^{Ph2} ligand								Dithiocarbamate ligand	
	5Ph (*o*)	5Ph (*m*)	5Ph (*p*)	3Ph (*o*)	3Ph (*m*)	3Ph (*p*)	4H	BH	N-CH$_2$	R
1	36.7	22.4	18.2	−73.5	3.7	3.8	49.0	119.1	101.6	32.4 (Me)
2	35.9	22.0	17.8	−71.2	3.2	3.9	49.8	115.6	93.3	36.9 (*o*-Ph), 15.2 (*m*-Ph), 13.8 (*p*-Ph)
3	36.6	22.3	18.1	−73.6	2.9	3.7	49.1	118.6	102.4	28.2 (CH$_2$)
4	7.7	7.0	7.4	4.8	6.9	7.2	59.3	−11.1	39.0	1.1 (Me)
5	7.8	7.1	7.4	4.7	6.7	7.1	61.0	−11.3	30.7	8.4 (*o*-Ph), 7.6 (*m*-Ph), 8.0 (*p*-Ph)
6	7.8	7.1	7.4	4.8	6.9	7.3	59.9	−10.9	38.8	4.9 (CH$_2$)

^{a} In CDCl$_3$.

^{1}H NMR spectroscopic studies

^{1}H NMR spectra of **1–6** were recorded in CDCl$_3$ and have been assigned by comparison with the previously reported [Tp^{Ph,Me}Ni(dtc)] (dtc = S$_2$CNEt$_2$, S$_2$CNPh$_2$) complexes and in the case of **1–3** with [Tp^{Ph,Me}Co(O–S)] (O–S = thiomalto-late, 1,2-hydroxypyridinethionate, 3,4-hydroxypyridinethionate),[8] [Tp^{Ph}Co(lactate)][29] and [Bp^{Ph2}Co{HB(3,5-pz^{Ph2})(pz^{Me2})$_2$}].[30] The ^{1}H NMR spectra reveal paramagnetically shifted resonances (Table 2) with the cobalt compounds exhibiting particularly large shifts over a range of 200 ppm (Fig. 2). The borohydride resonances are very broad and for **1–3** and **4–6** are found between 116 and 119 ppm and *ca.* −11 ppm, respectively. In both sets of complexes there is a single peak for the pyrazolyl protons indicative of fast rotation of the Tp^{Ph2} ligand. Such fluxional behaviour is well documented in first row transition metal Tp^R complexes.[1] For **1–3** the hydrogen atoms of the 3-phenyl ring are observed between −74 and −71 ppm, 2.9 and 3.7 ppm and 3.7 and 3.9 ppm for the *ortho*, *meta* and *para* protons, respectively. In contrast, the 5-phenyl ring protons are strongly deshielded and found between 17.8 and 36.7 ppm.

The nickel complexes exhibit similar resonances between 4.7 and 7.3 ppm and 7.1 and 7.8 ppm for the 3-phenyl and 5-phenyl protons, respectively. As with **1–3** the *ortho*-hydrogens of the 3-phenyl substituents are broad and shifted upfield of the other aromatic protons for the Tp^{Ph2} ligand. The dithiocarbamate ligand has sharp resonances for the N-C*H*$_2$R protons between 102 and 93 ppm and 39 and 31 ppm for **1–3** and **4–6**, respectively. Interestingly, in the case of the benzyl dithiocarbamate ligand the resonance is always *ca.* 9 ppm upfield of the other dithiocarbamates. The other protons for the dithiocarbamate ligands are readily identified and assigned based on their position and integration intensity, although the C*H*$_2$ protons for the pyrrolidine ring in **6** are found to overlap with *ortho* protons of the Tp^{Ph2} ligand.

X-ray crystallographic studies

The molecular structures of [Tp^{Ph2}Co(S$_2$CNEt$_2$)] **1**, [Tp^{Ph2}Co(S$_2$CN(CH$_2$)$_4$)] **3** and [Tp^{Ph2}Ni(S$_2$CN(CH$_2$)$_4$)] **6** have been determined by X-ray crystallography. Crystallographic data are presented in Tables 3 and 4 while the structures are shown in Fig. 3 and 4 for **1** and **6**, respectively. In the case of **3** and **6** two of the carbons in the pyrrolidine ring of the dithiocarbamate ligand are crystallographically disordered over two positions. All complexes show five-coordinate metal centres with κ^3 coordinated Tp^{Ph2} ligands and a geometry intermediate between square pyramidal and trigonal bipyramidal being slightly
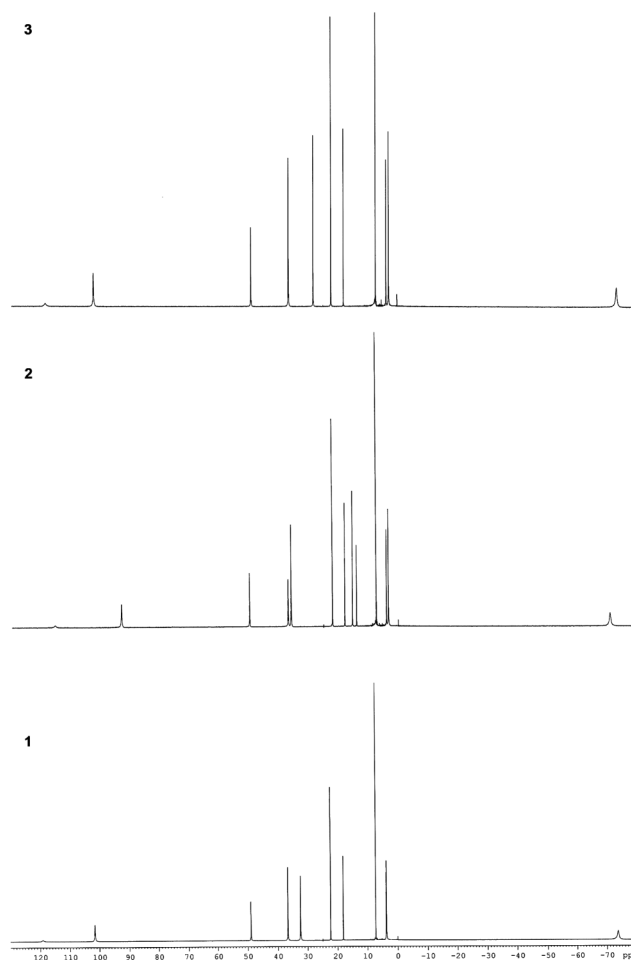
Fig. 2 ^{1}H NMR spectra of [Tp^{Ph2}Co(dtc)] **1–3**.

closer to the former. In contrast, the related [Tp^{Ph,Me}Ni(dtc)] (dtc = S$_2$CNEt$_2$, S$_2$CNPh$_2$) complexes are four-coordinate and square planar in the solid state, although a five-coordinate geometry exists in solution.[25] However, [Tp*Ni(S$_2$CNEt$_2$)][24] and the xanthate complex [Tp^{Ph,Me}Ni(S$_2$COEt)][25] are five-coordinate. In this instance it would appear that the more electron deficient Tp^{Ph2} ligand leads to coordination of the apical nitrogen in both the solid state and in solution while the more electron rich Tp^{Ph,Me} ligand is able to stabilize a four- rather than five-coordinate species.

The importance of steric effects is highlighted by [Tp*Ni(S$_2$CNEt$_2$)] which although more electron rich than both

Table 3 Bond lengths and angles for complexes **1**, **3** and **6**

	1	**3**	**6**	Tp*Ni(S₂CNEt₂)[a]
Bond lengths/Å				
M–N1	2.164(2)	2.0876(17)	2.049(2)	2.063(2)
M–N3	2.080(2)	2.1674(17)	2.085(2)	2.065(2)
M–N5	2.106(2)	2.0709(17)	2.051(2)	2.027(2)
M–S1	2.4267(8)	2.3676(10)	2.3510(9)	2.3747(8)
M–S2	2.3891(8)	2.4461(10)	2.4357(10)	2.4099(7)
C46–S1	1.716(3)	1.726(2)	1.696(3)	1.710(3)
C46–S2	1.735(3)	1.716(2)	1.715(3)	1.707(3)
C46–N7	1.335(3)	1.318(3)	1.322(4)	1.329(4)
Bond angles/°				
N1–M–N3	87.83(8)	81.47(6)	84.23(10)	88.39(8)
N1–M–N5	81.16(8)	95.75(7)	95.31(9)	93.47(9)
N3–M–N5	94.39(8)	87.56(7)	89.64(9)	88.68(8)
N3–M–S2	121.32(6)	171.78(4)	173.04(7)	171.95(6)
N5–M–S2	144.24(6)	100.51(5)	97.12(7)	98.19(6)
N1–M–S2	100.36(6)	99.13(5)	96.71(7)	95.33(6)
N3–M–S1	103.01(6)	99.57(5)	101.29(7)	99.59(6)
N5–M–S1	97.25(6)	119.97(5)	115.12(7)	112.05(7)
N1–M–S1	169.15(6)	144.27(5)	148.92(7)	153.27(7)
S1–M–S2	74.61(3)	75.11(2)	74.38(3)	73.99(3)
N7–C46–S1	122.0(2)	121.07(16)	121.7(3)	122.7(2)
N7–C46–S2	122.4(2)	121.90(16)	122.2(3)	122.4(2)
S1–C46–S2	115.54(15)	117.02(12)	116.11(19)	114.8(1)
τ[b]	0.42	0.46	0.40	0.31

[a] Data from ref. 24 [b] Ref. 31

Fig. 3 ORTEP diagram of [Tp^{Ph2}Co(S₂CNEt₂)] **1**, drawn with 50% ellipsoids.

Tp^{Ph2} and Tp^{Ph,Me} still results in a five-coordinate complex presumably due to the smaller steric bulk of Tp*. It is clear that a subtle combination of both steric and electronic effects influences the preferred coordinating mode of the Tp^R ligands in such dithiocarbamate complexes.

The Ni–N_{pz} and Ni–S bond lengths in **6** are very similar to those found in [Tp*Ni(S₂CNEt₂)] and [Tp^{PhMe}Ni(S₂COEt)] where the bond lengths are Ni–N_{pz} 2.042–2.078(2) Å; Ni–S1 2.399(1), Ni–S2 2.379(1) Å and Ni–N_{pz} 2.027–2.065(2) Å and Ni–S1 2.4099(7), Ni–S2 2.3747(8) Å, respectively, and are consistent with a paramagnetic Ni(II) centre.

On average the cobalt–nitrogen bond lengths are *ca.* 0.05 Å longer than in **6** and consistent with the different ionic radii of
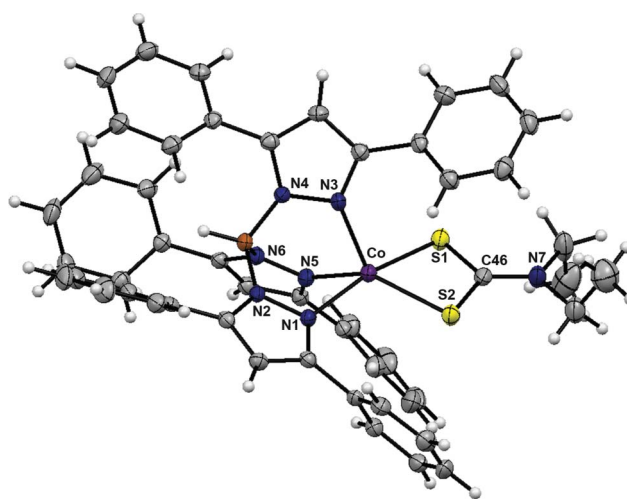
Co(II) and Ni(II).[32] A further difference between the cobalt and nickel complexes is that while the Tp^{Ph2} ligand is symmetrically coordinated in **6** one of the pyrazole arms of the Tp^{Ph2} ligand is elongated by between *ca.* 0.06–0.08 Å in **1** and **3** (see Table 3). Such asymmetric binding of the Tp^{Ph2} ligand has previously been observed in the structure of [Tp^{Ph2}Co(OAc)(Hpz^{Ph2})].[33] Furthermore, in all the complexes asymmetric binding of the dithiocarbamate is observed although the degree of asymmetry is dependent on the particular dithiocarbamate present. Thus ΔM–S = 0.038(1) Å for **1** and 0.079(1) and 0.085(1) Å for **3** and **6**, respectively. Interestingly, for [Tp*Ni(S₂CNEt₂)] ΔM–S = 0.035(1) Å suggesting that the constrained pyrrolidine dithiocarbamate ligand may cause asymmetric binding in Tp^R dithiocarbamate complexes. The dithiocarbamate ligands display small bite angles between 74.4 and 75.1° and similar to those reported for [Tp*Ni(S₂CNEt₂)] (73.99(3)°) and [Tp^{Ph,Me}Ni(S₂COEt)] (74.75(2)°).[24,25] The carbon–nitrogen and carbon–sulfur bond lengths are typical for bound dithiocarbamate ligands with values intermediate between those expected for carbon–element single and double bonds.

Table 4 Crystallographic data and structure refinement for complexes **1**, **3** and **6**

	1	**3**	**6**
Formula	C₅₀H₄₄BCoN₇S₂	C₅₀H₄₂BCoN₇S₂	C₅₀H₄₂BNiN₇S₂
Molecular weight/g mol⁻¹	876.78	874.77	874.55
Crystal system	Monoclinic	Monoclinic	Monoclinic
Space group	P2₁/c	P2₁/c	P2₁/c
a/Å	14.076(2)	13.960(5)	14.026(3)
b/Å	25.405(4)	25.122(10)	25.042(5)
c/Å	12.5980(19)	12.649(5)	12.672(2)
α/°	90	90	90
β/°	103.749(9)	102.047(5)	102.630(3)
γ/°	90	90	90
T/K	150(2)	150(2)	150(2)
Cell volume/Å³	4376.1(11)	4339(3)	4343.2(14)
Z	4	4	4
Absorption coefficient/mm⁻¹	0.532	0.536	0.587
Reflections collected	95001	38601	38822
Independent reflections, R_{int}	10063, 0.0990	8443, 0.0441	8434, 0.0594
Max. and min. transmission	0.9438 and 0.8234	0.8643 and 0.8060	0.8528 and 0.7905
Restraints/parameters	0/552	39/569	33/569
Final R indices [$I>2\sigma(I)$]:R_1, wR_2	0.0525, 0.1012	0.0364, 0.0888	0.0483, 0.1135
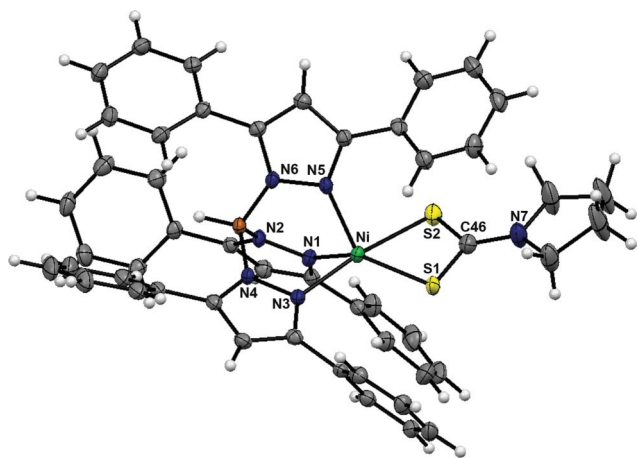
Fig. 4 ORTEP diagram of [Tp^{Ph2}Ni(S$_2$CN(CH$_2$)$_4$)] **6**, drawn with 50% ellipsoids.

Electrochemistry

Electrochemical studies reveal that both the Co and Ni complexes undergo *reversible* oxidation to Co(III) and Ni(III), respectively. The Co series are shown in Fig. 5 as representative examples. The reversibility of the redox couples of **4–6** matches those of the previously reported [Tp^{R}Ni(dtc)] (R = Ph,Me; Me$_2$) compounds.[24,25] It is noteworthy that the reduction of [Co(dtc)$_3$] to [Co(dtc)$_3$]$^-$ is quasi-reversible.[34] The cobalt complexes are *ca.* 80 mV more easily oxidized than the corresponding nickel compounds reflecting the greater stability of the Co(III) oxidation state (see Table 2). Surprisingly, the [Tp^{Ph2}Co(dtc)] complexes are more easily oxidized than the [Tp^{Ph2}Co(β-diketonate)] complexes by on average 750 mV.[23] This is extraordinary given that the only difference is the exchange of a β-diketonate ligand for a dithiocarbamate ligand. [Tp^{Ph2}Ni(S$_2$CNEt$_2$)] is found to be 130 mV more difficult to oxidize than [Tp^{Ph,Me}Ni(S$_2$CNEt$_2$)] indicating that substituents on the Tp^R ligand are able to influence the redox potential more than the dithiocarbamate ligands.[25] It may also explain the difficulty encountered in successfully synthesizing the [Tp^{Ph,Me}Co(dtc)] complexes noted earlier as these would be expected to be more easily oxidized than their Tp^{Ph2} counterparts.

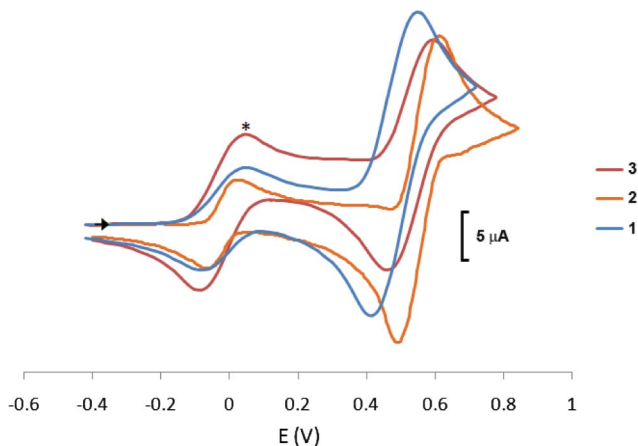**Fig. 5** Cyclic voltammograms of [Tp^{Ph2}Co(dtc) **1–3**, in CH$_2$Cl$_2$ at 100 mV s^{-1} (*[FeCp*$_2$]).

The complexes are oxidized in the order Et < pyr < Bz over a range of 70 mV suggesting that the substituent groups are also able to influence the oxidation potential and reflect the relative donor strength of the different dithiocarbamate ligands. The difference between the pyrrolidine and ethyl substituted dithiocarbamates is particularly interesting given that the ligands are so similar. This suggests that ring strain in the dithiocarbamate ligand may favour the dithiocarbamate resonance form over the thioureide form thereby reducing electron density at the metal (Fig. 6).
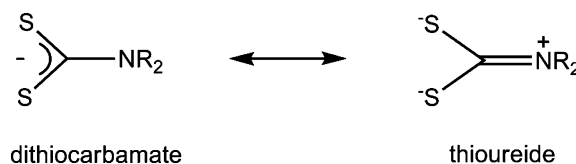

Fig. 6 Dithiocarbamate and thioureide resonance forms.

A decrease in the reduction potential of [Fe(S$_2$CNC$_4$H$_4$)$_3$] has also been ascribed to a decrease in the thioureide resonance form.[35]

Attempted oxidation of [Tp^{Ph2}Co(dtc)]

The oxidation potentials of **1–3** suggested that oxidation could be achieved using mild oxidizing agents. We therefore attempted the oxidation of [Tp^{Ph2}Co(dtc)] with acetyl ferrocenium, [FeCpCp^{COMe}]BF$_4$. The reaction proved to be not as simple as expected and after crystallization three products were evident. The first of these were colourless needles which proved to be Hpz^{Ph2} on the basis of IR and ^{1}H NMR spectroscopy. The other products were green and pink crystals. In the case of **2** we were able to structurally characterize one of these products. The crystals proved to be [Co(S$_2$CNBz$_2$)$_3$] with two molecules in the asymmetric unit (Fig. 7). The structure has previously been reported and the bond lengths and angles found in our structure are essentially identical.[36] The presence of free pyrazole in the reaction mixture and the pink colour of the crystals suggests that the final product may be [Tp^{Ph2}CoBp^{Ph2}]. A five-coordinate mixed pyrazole Tp^R and Bp^{Ph2} cobalt complex, [HB(pz^{Me2})$_2$(pz^{Ph2})CoBp^{Ph2}] has previously been prepared by Wołoweic *et al.* lending support to this hypothesis.[30]

DFT studies of [Tp^{Ph2}M(dtc)] complexes

In an attempt to better understand the remarkably low oxidation potential of the [Tp^{Ph2}M(dtc)] complexes and the instability of the [Tp^{Ph2}M(dtc)]$^+$ cations we have undertaken DFT calculations of the redox pairs [Tp^{Ph2}M(dtc)]$^{0/+}$. All calculations were performed using the Gaussian 03 software package with the B3LYP functional.[37]

The M–N and M–S bond lengths and the metal bond angles are close to those found in the structurally characterized compounds indicating that the models are accurate representations of [Tp^{Ph2}M(dtc)] (Table 5). Spin unrestricted calculations on the compounds reveal that the both the Co and Ni dithiocarbamate complexes are high spin being more stable than the corresponding low spin state by between 43.7–43.5 and 87.8–78.1 kJ mol^{-1} for the Co and Ni series, respectively. In the case of the [Tp^{Ph2}M(dtc)]$^+$ cations a singlet state is found for Ni indicating that it is low spin while for Co surprisingly a triplet state is found although it must

Table 5 Computed and X-ray crystallographically determined bond lengths for [Tp^{Ph2}M(dtc)] **1**, **3** and **6**

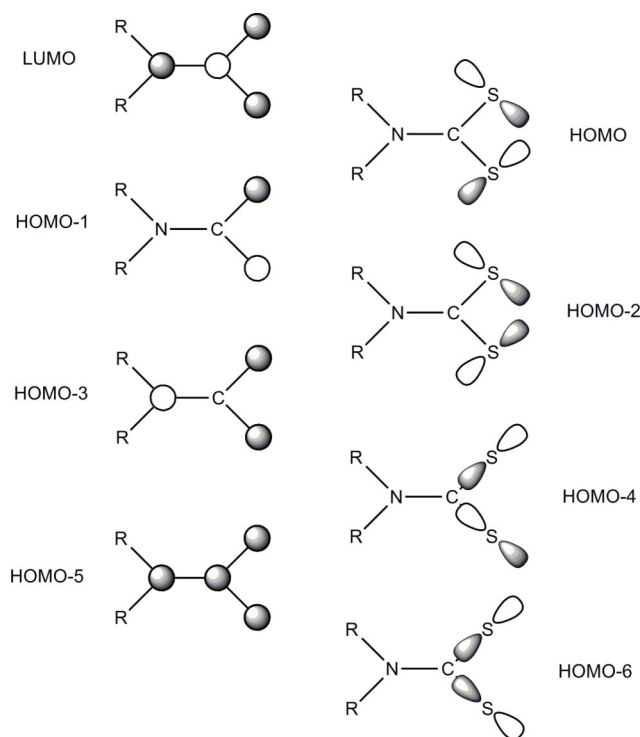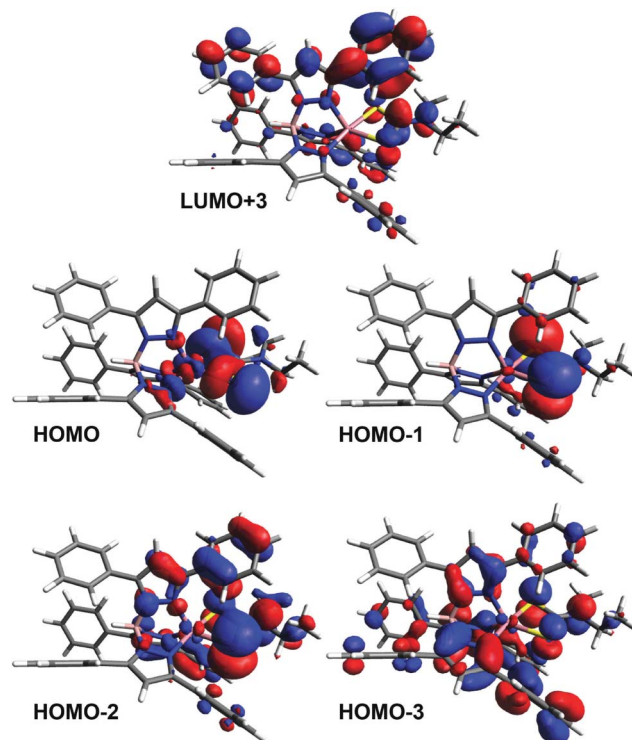|	1	1^a	3	3^a	6	6^a
Bond lengths/Å						
M–N1	2.164	2.171	2.0876	2.109	2.049	2.051
M–N3	2.080	2.077	2.1674	2.170	2.085	2.115
M–N5	2.106	2.110	2.0709	2.075	2.051	2.048
M–S1	2.4267	2.542	2.3676	2.462	2.3510	2.450
M–S2	2.3891	2.457	2.4461	2.548	2.4357	2.536
C46–S1	1.716	1.764	1.726	1.790	1.696	1.788
C46–S2	1.735	1.792	1.716	1.760	1.715	1.756
C46–N7	1.335	1.353	1.318	1.344	1.322	1.346

^{a} Computed value.
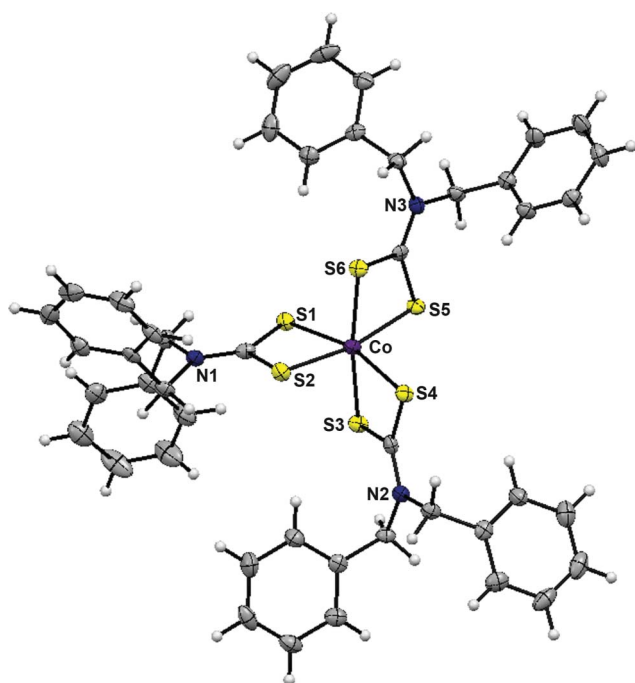
Fig. 7 ORTEP diagram of [Co(S$_2$CNBz$_2$)$_3$] drawn with 50% ellipsoids.

Fig. 8 Simplified dithiocarbamate molecular orbitals.

Fig. 9 Selected molecular orbitals of [Tp^{Ph2}Co(S$_2$CNEt$_2$)] **1** showing the M–S interactions.

be stated that B3LYP often overestimates the energy of different spin states.[38]

The eight principal orbitals that dithiocarbamate ligands possess in C_{2v} symmetry and which may be used in metal–ligand bonding have previously been described by Bitterwolf and are shown in Fig. 8.[39] Metal-dithiocarbamate bonding is thus described by a combination of these orbitals with suitable metal orbitals. In the present compounds the molecular orbitals concerning M–S interactions are shown in Fig. 9 for **1** as a representative example. The HOMO of all the complexes is found to be a strong M–S σ* interaction involving a metal d$_{x^2-y^2}$ and an asymmetric combination of the sulfur p$_x$ and p$_y$ orbitals (dtc HOMO in Fig. 8). The strong antibonding character of the orbital results in the HOMO being destabilised and therefore at high energy making oxidation comparatively easy.

As expected, the benzyl substituted dithiocarbamate complexes **2** and **5** are found to be stabilised relative to the ethyl and pyrrolidine substituted dithiocarbamate compounds consistent with the higher redox potential observed in the electrochemical studies. Interestingly, no significant difference in the energy

of the HOMO is observed between the ethyl and pyrrolidine substituted dithiocarbamate compounds despite there being a 50 mV difference in redox potential. The orbital immediately below the HOMO is composed of an asymmetric combination of the sulfur p$_z$ orbitals (dtc HOMO-1) and a metal d$_{xz}$ orbital

Dalton Trans. This journal is © The Royal Society of Chemistry 2011

resulting in a M–S π* interaction. The HOMO-2 also contains a M–S π* antibonding interaction constructed from a symmetric combination of the sulfur p_z orbitals (dtc HOMO-3) and a metal d_{yz} orbital. A weaker but almost identical M–S π* antibonding interaction, differing only in the inclusion of a strong M–Tp interaction, is found in the HOMO-3 orbital. The antibonding nature of all of the above interactions is consistent with the findings of Bitterwolf for [M(dtc)₂] (M = Ni, Cu, Zn) where the first three M–S interactions were all antibonding although the highest of these is empty in the case of the 16-electron Ni complex and thus forms the LUMO.[39] In addition, the metal d_{z^2} orbital is found in the HOMO-4 orbital and as with [Ni(dtc)₂] is non-bonding with respect to the dithiocarbamate ligand. The dithiocarbamate LUMO is located in the LUMO+3 orbital and is essentially a ligand π* orbital with no significant electron density on the metal. Once again a similar interaction is also observed in [Ni(dtc)₂]. These combined M–S interactions complete the picture of M–S bonding in the [Tp^{Ph2}M(dtc)] complexes.

In contrast to the M–S dominated HOMOs of the [Tp^{Ph2}M(dtc)] complexes the cations are radically different with only very weak M–S interactions in the frontier orbitals, HOMO to HOMO-8. However, as expected the LUMO is an antibonding M–S σ* orbital and similar to the HOMO found in the neutral complexes. The only other significant M–S interaction is the LUMO+1 which is a *π orbital containing the dithiocarbamate LUMO (dtc-LUMO Fig. 8) and a metal d_{yz} orbital. The lack of M–S interactions in the cations may explain the instability of the [Tp^{Ph2}M(dtc)]⁺ species as the dithiocarbamate ligand may be insufficiently bound resulting in loss of the ligand. This may also explain why the oxidation of [Tp^{Ph2}Co(dtc)] results in the formation of [Co(dtc)₃] and not the anticipated cation.

Conclusions

In conclusion, a series of novel Co and Ni tris(pyrazolyl)borate complexes have been prepared. The cobalt complexes, [Tp^{Ph2}Co(dtc)], are particularly notable being, to the best of our knowledge, the first *air stable* Co(II) dithiocarbamates not to employ soft phosphorous ligands. The Tp^{Ph2} ligand is crucial in the isolation of the cobalt compounds highlighting the importance of considering the electronic as well as steric properties of the Tp^R ligand. The complexes, [Tp^{Ph2}M(dtc)] adopt an intermediate coordination geometry between square pyramidal and trigonal bipyramidal and contrast with the related [Tp^{Ph,Me}Ni(dtc)] complexes which are diamagnetic and square planar; the coordination mode of the Tp^R ligand changing from κ³ to κ². Electrochemical studies indicate *reversible* oxidation to Co(III) and Ni(III) with the redox potential tunable over 80 mV by varying the substituents on the dithiocarbamate ligand. Oxidation of [Tp^{Ph2}Co(dtc)] with [FeCpCp^{COMe}]BF₄ yields [Co(dtc)₃], Hpz^{Ph2} and possibly [Tp^{Ph2}CoBp^{Ph2}]. DFT calculations indicate that the frontier orbitals of [Tp^{Ph2}M(dtc)] are dominated by the presence of M–S σ* and π* interactions. In contrast, the cations [Tp^{Ph2}M(dtc)]⁺ possess almost no M–S interactions perhaps explaining the instability of these complexes. Overall, the stability and ease with which these tris(pyrazolyl)borate dithiocarbamate complexes can be prepared and their high degree of tunability should allow the synthesis of more complex systems and efforts are in progress in our lab.

Experimental

General remarks

All manipulations were performed in air with HPLC grade solvents. Tris(3,5-diphenylpyrazolyl)borate (KTp^{Ph2}) was prepared by a literature procedure.[40] [Tp^{Ph2}MBr] were prepared as previously reported. All other chemicals were purchased from Fluka or Aldrich Chemical Company and used as received.

Infrared spectra (as KBr discs) were recorded on a Perkin-Elmer Spectrum One infrared spectrophotometer in the range 400–4000 cm⁻¹. Electronic spectra were recorded in CH₂Cl₂ at room temperature on a Shimadzu UV-1700 UV-Visible spectrophotometer. ¹H NMR spectra were recorded on a Bruker 300 MHz FT-NMR spectrometer at 25 °C in CDCl₃ with SiMe₄ added as an internal standard. Elemental analyses were carried out on a Eurovector EA3000 analyser. ESI-MS were carried out on a Bruker Daltonics 7.0T Apex 4 FTICR Mass Spectrometer. Electrochemical studies were carried out using a palmsens PC *vs.* 2.11 potentiosat in conjunction with a three-electrode cell. The auxiliary electrode was a platinum rod and the working electrode was a platinum disc (2.0 mm diameter). The reference electrode was a Ag–AgCl electrode. Solutions in CH₂Cl₂ dried over CaH₂, were 5×10^{-4} mol dm⁻³ in the test compound and 0.1 mol dm⁻³ in [NBuⁿ₄][PF₆] as the supporting electrolyte. Under these conditions, $E^{0'}$ for the one-electron oxidation of [Fe(η-C₅H₅)₂] added to the test solutions as an internal calibrant is 0.52 V.

Synthesis of complexes

Synthesis of [Tp^{Ph2}Co(S₂CNEt₂)] 1. [Tp^{Ph2}CoBr] (81 mg, 0.1 mmol) was suspended in CH₂Cl₂ (10 ml) giving a turquoise suspension. NaS₂CNEt₂ (24 mg, 0.1 mmol) was added resulting in a change of colour to brown. The solution was stirred for 5 h and reduced to dryness *in vacuo*. The solid was redissolved in CH₂Cl₂ (2 ml) and layered with hexanes (15 ml). After 2 days purple-brown crystals formed which were washed with Et₂O (2 × 5 ml) and air dried (56 mg, 63%). ν_{max} (KBr)/cm⁻¹ 3055, 2973, 2931 (ν_{CH}), 2623 (ν_{BH}), 1478 ($\nu_{C=N}$), 1010 (ν_{CS}). ¹H NMR (CDCl₃, 295 K; δ; ppm) 119.1 (1H, BH), 101.6 (4H, N-CH₂), 49.0 (3H, 4-pz), 36.7 (6H, 5-*o*-Ph), 32.4 (6H, Me), 22.4 (6H, 5-*m*-Ph), 18.2 (3H, 5-*p*-Ph), 3.8 (3H, 3-*p*-Ph), 3.7 (6H, 3-*m*-Ph), −73.5 (6H, 3-*o*-Ph). UV-Vis λ_{max}(CH₂Cl₂)/nm (ε, dm³ mol⁻¹ cm⁻¹) 408 (859), 536 (63). m/z (ESI) 728 [M − S₂CNEt₂]⁺. Anal. Calc. for C₅₀H₄₄N₇BS₂Co: C 68.49, H 5.06, N 11.18; Found: C 68.35, H 5.02, N 11.13.

Complexes **2–6** were synthesized in a similar manner to **1** using appropriate cobalt or nickel starting materials and recrystallized from the solvents indicated.

Synthesis of [Tp^{Ph2}Co(S₂CNBz₂)] 2. Purple-brown crystals (crystallised from CH₂Cl₂-hexane). 69% yield. ν_{max} (KBr)/cm⁻¹ 3056, 3027, 2937 (ν_{CH}), 2613 (ν_{BH}), 1475 ($\nu_{C=N}$), 1009 (ν_{CS}). ¹H NMR (CDCl₃, 295 K; δ; ppm) 115.6 (1H, BH), 93.3 (4H, N-CH₂), 49.8 (3H, 4-pz), 36.9 (4H, dtc-*o*-Ph), 35.9 (6H, 5-*o*-Ph), 22.0 (6H, 5-*m*-Ph), 17.8 (3H, 5-*p*-Ph), 15.2 (4H, dtc-*m*-Ph), 13.8 (2H, dtc-*p*-Ph), 3.9 (3H, 3-*p*-Ph), 3.2 (6H, 3-*m*-Ph), −71.2 (6H, 3-*o*-Ph). UV-Vis λ_{max} (CH₂Cl₂)/nm (ε, dm³ mol⁻¹ cm⁻¹) 404 (974), 535 (72). m/z (ESI) 728 [M − S₂CNBz₂]⁺. Anal. Calc. for C₆₀H₄₈N₇BS₂Co: C 72.00, H 4.83, N 9.80; Found: C 71.67, H 4.84, N 9.79.

Synthesis of [Tp^{Ph2}Co(S$_2$CN(CH$_2$)$_4$)] 3. Purple crystals (crystallised from CH$_2$Cl$_2$-hexane). 64% yield. v_{max} (KBr)/cm^{-1} 3058, 2970 (v_{CH}), 2626 (v_{BH}), 1479 ($v_{C=N}$), 1011 (v_{CS}). ^{1}H NMR (CDCl$_3$, 295 K; δ; ppm) 118.6 (1H, BH), 102.4 (4H, N-CH$_2$), 49.1 (3H, 4-pz), 36.6 (6H, 5-o-Ph), 28.2 (4H, CH$_2$), 22.3 (6H, 5-m-Ph), 18.1 (3H, 5-p-Ph), 3.7 (3H, 3-p-Ph), 2.9 (6H, 3-m-Ph), −73.6 (6H, 3-o-Ph). UV-Vis λ_{max}(CH$_2$Cl$_2$)/nm (ε, dm^3 mol^{-1} cm^{-1}) 402 (1,071), 505 (73). m/z (ESI) 728 [M − S$_2$CN(CH$_2$)$_4^-$]$^+$. Anal. Calc. for C$_{50}$H$_{42}$N$_7$BS$_2$Co: C 68.65, H 4.84, N 11.21; Found: C 68.84, H 5.01, N 11.19.

Synthesis of [Tp^{Ph2}Ni(S$_2$CNEt$_2$)] 4. Green crystals (crystallised from CH$_2$Cl$_2$–hexane). 85% yield. v_{max}(KBr)/cm^{-1} 3054, 2972, 2930 (v_{CH}), 2624 (v_{BH}), 1478 ($v_{C=N}$), 1011 (v_{CS}). ^{1}H NMR (CDCl$_3$, 295 K; δ; ppm) 59.3 (3H, 4-pz), 39.0 (4H, N-CH$_2$), 7.7 (6H, 5-o-Ph), 7.4 (3H, 5-p-Ph), 7.2 (3H, 3-p-Ph), 7.0 (6H, 5-m-Ph), 6.9 (6H, 3-m-Ph), 4.8 (6H, 3-o-Ph), 1.1 (6H, Me), −11.1 (1H, BH). UV-Vis λ_{max}(CH$_2$Cl$_2$)/nm (ε, dm^3 mol^{-1} cm^{-1}) 372sh (1,460), 426 (1,190), 654 (95). m/z (ESI) 727 [M − S$_2$CNEt$_2^-$]$^+$. Anal. Calc. for C$_{50}$H$_{44}$N$_7$BS$_2$Ni: C 68.51, H 5.06, N 11.19; Found: C 68.33, H 4.94, N 11.14.

Synthesis of [Tp^{Ph2}Ni(S$_2$CNBz$_2$)] 5. Green crystals (crystallised from CH$_2$Cl$_2$-hexane). 84% yield. v_{max}(KBr)/cm^{-1} 3059, 3025, 2910 (v_{CH}), 2610 (v_{BH}), 1471 ($v_{C=N}$), 1011 (v_{CS}). ^{1}H NMR (CDCl$_3$, 295 K; δ; ppm) 61.0 (3H, 4-pz), 30.7 (4H, N-CH$_2$), 8.4 (4H, dtc-o-Ph), 8.0 (2H, dtc-p-Ph), 7.8 (6H, 5-o-Ph), 7.6 (4H, dtc-m-Ph), 7.4 (3H, 5-p-Ph), 7.1 (9H, 3-p-Ph and 5-m-Ph), 6.7 (6H, 3-m-Ph), 4.7 (6H, 3-o-Ph), −11.3 (1H, BH). UV-Vis λ_{max}(CH$_2$Cl$_2$)/nm (ε, dm^3 mol^{-1} cm^{-1}) 365sh (1,860), 426 (1,187), 655 (103). m/z (ESI) 727 [M − S$_2$CNBz$_2^-$]$^+$. Anal. Calc. for C$_{60}$H$_{48}$N$_7$BS$_2$Ni: C 72.01, H 4.83, N 9.80; Found: C 71.88, H 4.79, N 9.72.

Synthesis of [Tp^{Ph2}Ni(S$_2$CN(CH$_2$)$_4$)] 6. Green crystals (crystallised from CH$_2$Cl$_2$–hexane). 77% yield. v_{max} (KBr)/cm^{-1} 3058, 2969, 2869 (v_{CH}), 2626 (v_{BH}), 1479 ($v_{C=N}$), 1011 (v_{CS}). ^{1}H NMR (CDCl$_3$, 295 K; δ; ppm) 59.9 (3H, 4-pz), 38.8 (4H, N-CH$_2$), 7.8 (6H, 5-o-Ph), 7.4 (3H, 5-p-Ph), 7.3 (3H, 3-p-Ph), 7.1 (6H, 5-m-Ph), 6.9 (6H, 3-m-Ph), 4.9 (4H, CH$_2$), 4.8 (6H, 3-o-Ph), −10.9 (1H, BH). UV-Vis λ_{max} (CH$_2$Cl$_2$)/nm (ε, dm^3 mol^{-1} cm^{-1}) 372sh, (1,360), 429 (1,011), 658 (95). m/z (ESI) 727 [M − S$_2$CN(CH$_2$)$_4^-$]$^+$. Anal. Calc. for C$_{50}$H$_{42}$N$_7$BS$_2$Ni: C 68.67, H 4.84, N 11.21; Found: C 68.74, H 4.77, N 11.43.

X-ray crystallography. Crystal data and data processing parameters for the structures of **1**, **3** and **6** are given in Tables 2 and 3. X-ray quality crystals of **1**, **3** and **6** were grown by allowing hexane to diffuse into a concentrated solution of the complex in CH$_2$Cl$_2$. Crystals were mounted on a glass fibre using perfluoropolyether oil and cooled rapidly to 150 K in a stream of cold nitrogen. All diffraction data were collected on a Bruker Smart CCD area detector with graphite monochromated Mo Kα (λ = 0.71073 Å). After data collection, in each case an empirical absorption correction (SADABS) was applied,[41] and the structures were then solved by direct methods and refined on all F^2 data using the SHELX suite of programs.[42] In all cases non-hydrogen atoms were refined with anisotropic thermal parameters; hydrogen atoms were included in calculated positions and refined with isotropic thermal parameters which were $ca.$ 1.2 × (aromatic CH, CH$_2$) or 1.5 × (Me) the equivalent isotropic thermal parameters of their parent carbon atoms.

Computational details. All calculations were performed with Gaussian 03 (Revision B.04)[43] and used the B3LYP density functional. The structural properties of the complexes obtained from X-ray crystallographic data were used as initial structures for full optimization. Calculations were performed at the DFT-B3LYP level of theory using an SDD basis set. Geometry optimizations were performed in the gas phase for each given spin state. The molecular orbital analyses were then conducted at those geometries. The HOMO and LUMO three-dimensional isosurface plots were generated using Avogadro.[44]

Notes and references

1 S. Trofimenko, *Scorpionates: The Coordination Chemistry of Polypyrazolylborate Ligands*, Imperial College Press, London, 1999.
2 S. Trofimenko, *Chem. Rev.*, 1993, **93**, 943.
3 J. C. Calabrese, S. Trofimenko and J. S. Thompson, *J. Chem. Soc., Chem. Commun.*, 1986, 1122.
4 S. Trofimenko, J. C. Calabrese, P. J. Domaille and J. S. Thompson, *Inorg. Chem.*, 1987, **26**, 1507.
5 S. Trofimenko, J. C. Calabrese and J. S. Thompson, *Inorg. Chem.*, 1989, **28**, 1091.
6 S. Trofimenko, J. C. Calabrese, J. K. Kochi, S. Wolowiec, F. B. Hulsbergen and J. Reedijk, *Inorg. Chem.*, 1992, **31**, 3943.
7 A. Kremer-Aach, W. Kläui, R. Bell, A. Strerath, H. Wunderlich and D. Mootz, *Inorg. Chem.*, 1997, **36**, 1552.
8 F. E. Jacobsen, R. M. Breece, W. K. Myers, D. L. Tierney and S. M. Cohen, *Inorg. Chem.*, 2006, **45**, 7306.
9 R. Han, A. Looney, K. McNeill, G. Parkin, A. L. Rheingold and B. S. Haggerty, *J. Inorg. Biochem.*, 1993, **49**, 105.
10 C. Bergquist, T. Fillebeen, M. M. Morlok and G. Parkin, *J. Am. Chem. Soc.*, 2003, **125**, 6189.
11 Y. Matsunaga, K. Fujisawa, N. Ibi, Y. Miyashita and K. Okamoto, *Inorg. Chem.*, 2005, **44**, 325.
12 S. I. Gorelsky, L. Basumallick, J. Vura-Weis, R. Sarangi, K. O. Hodgson, B. Hedman, K. Fujisawa and E. I. Solomon, *Inorg. Chem.*, 2005, **44**, 4947.
13 K. Fujisawa, T. Kakizaki, Y. Miyashita and K. Okamoto, *Inorg. Chim. Acta*, 2008, **361**, 1134.
14 N. Shirasawa, T. T. Nguyet, S. Hikichi, Y. Moro-oka and M. Akita, *Organometallics*, 2001, **20**, 3582.
15 N. Shirasawa, M. Akita, S. Hikichi and Y. Moro-oka, *Chem. Commun.*, 1999, 417.
16 S. Yoshimitsu, S. Hikichi and M. Akita, *Organometallics*, 2002, **21**, 3762.
17 M. Akita, *J. Organomet. Chem.*, 2004, **689**, 4540 and references therein.
18 A. S. Yakovenko, S. V. Kolotilov, A. W. Addison, S. Trofimenko, G. P. A. Yap, V. Lopushanskaya and V. V. Pavlishchuk, *Inorg. Chem. Commun.*, 2005, **8**, 932.
19 J. W. Egan, B. S. Haggerty, A. L. Rheingold, S. C. Sendlinger and K. H. Theopold, *J. Am. Chem. Soc.*, 1990, **112**, 2445.
20 J. L. Detrich, R. Konecny, W. M. Vetter, D. Doren, A. L. Rheingold and K. H. Theopold, *J. Am. Chem. Soc.*, 1996, **118**, 1703.
21 J. D. Jewson, L. M. Liable-Sands, G. P. A. Yap, A. L. Rheingold and K. H. Theopold, *Organometallics*, 1999, **18**, 300.
22 S. Hikichi, M. Yoshizawa, Y. Sasakura, H. Komatsuzaki, Y. Moro-oka and M. Akita, *Chem.–Eur. J.*, 2001, **7**, 5011.
23 D. J. Harding, P. Harding, R. Daengngern, S. Yimklan and H. Adams, *Dalton Trans.*, 2009, 1314.
24 H. Ma, G. Wang, G. T. Yee, J. L. Petersen and M. P. Jensen, *Inorg. Chim. Acta*, 2009, **362**, 4563.
25 H. Ma, S. Chattopadhyay, J. L. Petersen and M. P. Jensen, *Inorg. Chem.*, 2008, **47**, 7966.

26 G. Hogarth, *Prog. Inorg. Chem.*, 2005, **53**, 71.

27 K. Nakamoto, *in Infrared and Raman Spectra of Inorganic and Coordination Compounds: Part B*, 5th edn, John Wiley & Sons, New York, 1997, pp. 91–99.

28 P. J. Desrochers, R. W. Cutts, P. K. Rice, M. L. Golden, J. B. Graham, T. M. Barclay and A. W. Cordes, *Inorg. Chem.*, 1999, **38**, 5690.

29 M. Łukasiewicz, Z. Ciunik and S. Wołowiec, *Polyhedron*, 2000, **19**, 2119.

30 T. Ruman, Z. Ciunik, J. Mazurek and S. Wołowiec, *Eur. J. Inorg. Chem.*, 2002, 754.

31 A. W. Addison, T. N. Rao, J. Reedijk, J. Van Rijn and G. C. Verschoor, *J. Chem. Soc., Dalton Trans.*, 1984, 1349.

32 F. A. Cotton, G. Wilkinson, C. A. Murillo and M. Bochmann, *Advanced Inorganic Chemsitry*, 6th edn, John Wiley & Sons, New York, 1999, p. 1304.

33 D. J. Harding, H. Adams and T. Tuntulani, *Acta Crystallogr., Sect. C: Cryst. Struct. Commun.*, 2005, **61**, m301.

34 H. T. V. Hoa and R. J. Magee, *J. Inorg. Nucl. Chem.*, 1979, **41**, 351.

35 A. G. El A'mma and R. S. Drago, *Inorg. Chem.*, 1977, **16**, 2975.

36 P. C. Healy, J. W. Connor, B. W. Skelton and A. H. White, *Aust. J. Chem.*, 1990, **43**, 1083.

37 M. J. Frisch *et al.*, *GAUSSIAN 03, revision C02*, Gaussian, Inc.: Wallingford CT, 2004.

38 H. Paulsen and A. X. Trautwein, *Top. Curr. Chem.*, 2004, **235**, 197 and references therein.

39 T. E. Bitterwolf, *Inorg. Chim. Acta*, 2008, **361**, 1319.

40 N. Kitajima, K. Fujisawa, C. Fujimoto, Y. Moro-oka, S. Hashimoto, T. Kitagawa, K. Toriumi, K. Tatsumi and A. Nakamura, *J. Am. Chem. Soc.*, 1992, **114**, 1277.

41 *Bruker, SMART, XSCANS, SHEXTL and SADABS*, Bruker AXS Inc., Madison, Wisconsin, USA, 2005.

42 G. M. Sheldrick, *SHELXS97* and SHELXL97. University of Göttingen, Germany, 1997.

43 M. J. Frisch, G. W. Trucks, H. B. Schlegel, G. E. Scuseria, M. A. Robb, J. R. Cheeseman, J. A. Montgomery Jr., T. Vreven, K. N. Kudin, J. C. Burant, J. M. Millam, S. S. Iyengar, J. Tomasi, V. Barone, B. Mennucci, M. Cossi, G. Scalmani, N. Rega, G. A. Petersson, H. Nakatsuji, M. Hada, M. Ehara, K. Toyota, R. Fukuda, J. Hasegawa, M. Ishida, T. Nakajima, Y. Honda, O. Kitao, H. Nakai, M. Klene, X. Li, J. E. Knox, H. P. Hratchian, J. B. Cross, V. Bakken , C. Adamo, J. Jaramillo, R. Gomperts, R. E. Stratmann, O. Yazyev, A. J. Austin, R. Cammi, C. Pomelli, J. W. Ochterski, P. Y. Ayala, K. Morokuma, G. A. Voth, P. Salvador, J. J. Dannenberg, V. G. Zakrzewski, S. Dapprich, A. D. Daniels, M. C. Strain, O. Farkas, D. K. Malick, A. D. Rabuck, K. Raghavachari, J. B. Foresman, J. V. Ortiz, Q. Cui, A. G. Baboul, S. Clifford, J. Cioslowski, B. B. Stefanov, G. Liu, A. Liashenko, P. Piskorz, I. Komaromi, R. L. Martin, D. J. Fox, T. Keith, M. A. Al-Laham, C. Y. Peng, A. Nanayakkara, M. Challacombe, P. M. W. Gill, B. Johnson, W. Chen, M. W. Wong, C. Gonzalez; and J. A. Pople, *Gaussian 03, Revision B.04*, Gaussian, Inc., Pittsburgh PA, 2003.

44 http://avogadro.openmolecules.net/accessed 18/06/2010.